

**GREEN SYNTHESIS OF SILVER  
NANOPARTICLES FROM WATER-SOLUBLE  
POLYSACCHARIDES OF *CLINACANTHUS  
NUTANS* LEAF: EXTRACTION,  
CHARACTERISATION, OPTIMISATION AND  
ANTIBACTERIAL STUDIES**

**KOGILAVANEE A/P DEVASVARAN**

**UNIVERSITI SAINS MALAYSIA**

**2023**

**GREEN SYNTHESIS OF SILVER  
NANOPARTICLES FROM WATER-SOLUBLE  
POLYSACCHARIDES OF *CLINACANTHUS  
NUTANS* LEAF: EXTRACTION,  
CHARACTERISATION, OPTIMISATION AND  
ANTIBACTERIAL STUDIES**

by

**KOGILAVANEE A/P DEVASVARAN**

**Thesis submitted in fulfilment of the requirements  
for the degree of  
Doctor of Philosophy**

**July 2023**

## ACKNOWLEDGEMENT

Firstly, I am forever thankful to my supervisor Assoc Prof ChM. Dr Lim Vuanghao for being supportive, responsive and an excellent advisor throughout my PhD journey. Without him, I wouldn't have had the opportunity of conducting my research project or develop independence and confidence in executing the project. I am also thankful to my co-supervisors, Dr Muhammad Amir bin Yunus, for his guidance, advice and checking of part of my dissertation, and to Dr Nik Nur Syazni Binti Nik Mohamed Kamal. I also sincerely appreciate Dr Citartan Marimuthu for his invaluable advice on my project. I am forever grateful for having such wonderful colleagues, especially; Batoul Alallam, Mustahimah, Peter Justin, Dr Hakimin, Vasagee and Ravi Kumar, for their resourcefulness, kindness, and support throughout my PhD journey. Moreover, I would like to express my sincere gratitude to all the staffs at Universiti Sains Malaysia (USM) for their hospitable nature and assistance throughout my study. Furthermore, I would like to acknowledge USM for awarding me with the GRA-Assist scholarship in my first semester and the GA-Scholarship for the complete duration of my study. Last but not least, I am immensely grateful to my family; Devasvaran, Vimala Devi, Deeba, Subha, Viji, Vignes, Naavin, Usha, Uma, Sandha Sandhini and Bilbo, for their continuous encouragement and support throughout my PhD journey. I couldn't have done it without them.

## TABLE OF CONTENTS

<b>ACKNOWLEDGEMENT</b> .....	<b>ii</b>
<b>TABLE OF CONTENTS</b> .....	<b>iii</b>
<b>LIST OF TABLES</b> .....	<b>xi</b>
<b>LIST OF FIGURES</b> .....	<b>xiv</b>
<b>LIST OF SYMBOLS</b> .....	<b>xxii</b>
<b>LIST OF ABBREVIATIONS</b> .....	<b>xxiii</b>
<b>LIST OF APPENDICES</b> .....	<b>xxvi</b>
<b>ABSTRAK</b> .....	<b>xxvii</b>
<b>ABSTRACT</b> .....	<b>xxix</b>
<b>CHAPTER 1 INTRODUCTION</b> .....	<b>1</b>
1.1 Research background .....	1
1.2 Problem statements .....	5
1.3 Research hypothesis .....	6
1.4 Research questions .....	7
1.5 Research aim and objectives .....	7
1.5.1 Objectives.....	7
1.6 Significance of the study .....	8
1.7 Flow chart of the study .....	9
<b>CHAPTER 2 LITERATURE REVIEW</b> .....	<b>10</b>
2.1 <i>Clinacanthus nutans</i> ( <i>C. nutans</i> ) .....	10
2.1.1 <i>C. nutans</i> phytochemical compounds.....	11
2.1.2 <i>C. nutans</i> pharmacological activities .....	12
2.2 Carbohydrates.....	14
2.2.1 Crude polysaccharides.....	15

2.2.1(a)	Extraction of water-soluble crude polysaccharides from plants .....	17
2.2.1(b)	Solubility.....	19
2.2.1(c)	Antioxidant activities.....	20
2.3	Metabolomics .....	22
2.4	Silver nanoparticles (AgNP) .....	25
2.4.1	General routes for AgNP synthesis .....	26
2.4.1(a)	Physical route of AgNP synthesis.....	28
2.4.1(b)	Chemical route of AgNP synthesis.....	29
2.4.1(c)	Biological route of AgNP synthesis .....	29
2.4.2	Microwave-assisted green synthesis .....	35
2.4.3	Polysaccharides as a reducing agent .....	36
2.4.3(a)	Mechanism of saccharide as a reducing agent.....	37
2.4.4	Characterisation of AgNP .....	39
2.4.4(a)	Ultraviolet-visible spectroscopy (UV-Vis).....	39
2.4.4(b)	Dynamic light scattering (DLS).....	40
2.4.4(c)	Attenuated total reflectance-Fourier transform infrared spectroscopy (ATR-FTIR).....	41
2.4.4(d)	X-ray diffractometry analysis (XRD).....	41
2.4.4(e)	Scanning electron microscopy (SEM).....	42
2.4.4(f)	Transmission electron microscopy (TEM) .....	43
2.4.5	Biological activities of green synthesised AgNP .....	43
2.4.5(a)	Antibacterial activities of crude polysaccharide synthesised AgNP .....	43
2.4.5(b)	AgNP antibacterial mechanism of action .....	45
2.5	Brine shrimp lethality bioassay .....	49
2.6	Bacteria.....	49
2.6.1	<i>Staphylococcus aureus</i> ( <i>S. aureus</i> ) .....	51

2.6.2	<i>Escherichia coli</i> ( <i>E. coli</i> ).....	52
2.7	Antibiotics .....	52
2.7.1	Quinolones .....	54
2.7.2	Ciprofloxacin.....	58
2.8	Statistical analysis .....	60
2.8.1	Statistical product and service solutions (SPSS).....	60
2.8.2	Multivariate data analysis.....	61
2.8.2(a)	Response surface method (RSM) .....	61
2.8.2(b)	Metabolomics data.....	64
<b>CHAPTER 3 MATERIALS &amp; METHODS.....</b>		<b>66</b>
3.1	Materials.....	67
3.2	<i>Clinacanthus nutans</i> ( <i>C. nutans</i> ) leaf.....	69
3.3	<i>C. nutans</i> leaf crude polysaccharide (CNP) extraction .....	70
3.3.1	Hot water extraction (HW_CNP) method.....	70
3.3.2	Ultrasound-assisted extraction (UL_CNP) method.....	70
3.3.3	Freeze-thaw extraction (FT_CNP) method.....	71
3.3.4	Alkaline extraction (ALK_CNP) method .....	71
3.3.5	Acid extraction (ACD_CNP) method .....	71
3.4	Single-factor optimisation of CNP extraction .....	71
3.5	Characterisation of CNP.....	72
3.5.1	Determination of total carbohydrate content.....	72
3.5.2	Determination of total protein content .....	72
3.5.3	Determination of total phenolic content.....	73
3.6	Antioxidant activity of CNP.....	73
3.6.1	2,2-diphenyl-1-picryl-hydrazyl-hydrate (DPPH) radical scavenging assay .....	73
3.6.2	2,2'-azino-bis(3-ethylbenzothiazoline-6-sulfonic acid) (ABTS) radical scavenging assay .....	74

3.7	Composition analysis of CNP .....	74
3.7.1	Attenuated total reflectance-Fourier transform infrared spectroscopy (ATR-FTIR) chemometrics .....	75
3.7.2	Gas chromatography-mass spectrometry (GC-MS).....	75
3.7.3	GC-MS-metabolomics sample preparation .....	76
3.8	Silver nanoparticles (AgNP) characterisation .....	77
3.8.1	Silver nanoparticles (AgNP) synthesis.....	78
3.8.2	Silver nanoparticles (AgNP) synthesis optimisation.....	78
3.8.3	Conjugation efficiency .....	80
3.8.4	Ultraviolet-visible spectroscopy (UV-Vis) .....	80
3.8.5	Attenuated total reflectance-Fourier transform infrared spectroscopy (ATR-FTIR) .....	80
3.8.6	Zeta potential, hydrodynamic size and size distribution .....	81
3.8.7	X-ray diffractometry analysis (XRD) .....	81
3.8.8	Scanning electron microscopy (SEM) with energy dispersive X-ray analysis (EDX).....	81
3.8.9	Transmission electron microscopy (TEM).....	82
3.9	Brine shrimp (in vivo) lethality bioassay .....	82
3.10	Bacterial sample preparation .....	83
3.10.1	Bacterial strains .....	83
3.10.2	Preparation of media .....	84
3.10.3	Preparation of bacterial cultures.....	84
3.11	Antibacterial activity .....	84
3.11.1	Kirby-Bauer disk diffusion assay .....	85
3.11.2	Broth microdilution assay .....	85
3.11.3	Time-kill kinetics assay.....	86
3.12	Identification of target genes using polymerase chain reaction (PCR) .....	87
3.12.1	Complete genome of <i>E. coli</i> and <i>S. aureus</i> .....	87

3.12.2	Nucleotide sequence.....	87
3.12.3	Primer design.....	87
3.12.4	Oligonucleotide synthesis .....	87
3.12.5	Genomic DNA extraction.....	89
3.12.6	DNA concentration and purity .....	90
3.12.7	Polymerase chain reaction (PCR) .....	90
3.12.8	Agarose gel electrophoresis and gel imaging.....	90
3.13	Bacterial gene expression study utilising real-time PCR.....	91
3.13.1	Bacterial cell treatment.....	91
3.13.2	RNA extraction .....	91
3.13.3	RNA concentration and purity .....	92
3.13.4	Two-step real-time quantitative PCR.....	92
3.13.5	cDNA synthesis.....	92
3.13.6	Quantitative polymerase chain reaction (qPCR).....	93
3.14	Statistical analysis .....	93
<b>CHAPTER 4 RESULTS AND DISCUSSION.....</b>		<b>94</b>
4.1	Single-factor optimisation of <i>C. nutans</i> leaf crude polysaccharide (CNP) extraction.....	94
4.1.1	Hot water extraction (HW_CNP).....	95
4.1.2	Ultrasound-assisted extraction (UL_CNP).....	97
4.1.3	Freeze-thaw extraction (FT_CNP).....	99
4.1.4	Alkaline extraction (ALK_CNP) .....	100
4.1.5	Acid extraction (ACD_CNP) .....	101
4.1.6	Summary of the percentage yield of the CNP extraction methods .....	103
4.2	Characterisation of CNP.....	104
4.2.1	Total carbohydrate content.....	104
4.2.2	Total protein content .....	106



4.2.3	Total phenolic content.....	107
4.2.4	Antioxidant activity.....	109
4.2.4(a)	2,2-diphenyl-1-picryl-hydrazyl-hydrate (DPPH) radical scavenging .....	109
4.2.4(b)	2,2'-azino-bis(3-ethylbenzothiazoline-6-sulfonic acid (ABTS) radical scavenging.....	113
4.2.5	Correlation of TPC with DPPH and ABTS.....	115
4.3	Composition analysis of CNP by FTIR and GC-MS .....	116
4.3.1	Attenuated total reflectance-Fourier transform infrared spectroscopy (ATR-FTIR) chemometrics.....	116
4.3.1(a)	Classification of CNP by unsupervised principal component analysis (PCA) .....	118
4.3.1(b)	Correlation of CNP with antioxidant activities by partial least square (PLS).....	120
4.3.2	Gas chromatography-mass spectrometry (GC-MS).....	125
4.3.2(a)	Untargeted metabolite profiling using GC-MS .....	131
4.4	Silver nanoparticle (AgNP) synthesis optimisation .....	134
4.4.1	ALK_CNP synthesised silver nanoparticles (ALK_AgNP) .....	134
4.4.1(a)	Optimisation of ALK_AgNP synthesis .....	136
4.4.1(b)	Fitting the model.....	136
4.4.1(c)	Effect of independent variables on the nanoparticle size of ALK_AgNP.....	138
4.4.1(d)	Effect of independent variables on the conjugation efficiency of ALK_AgNP .....	140
4.4.1(e)	Verification of the optimised solution generated by the RSM .....	142
4.4.2	ACD_CNP synthesised silver nanoparticles (ACD_AgNP).....	143
4.4.2(a)	Optimisation of ACD_AgNP synthesis .....	144
4.4.2(b)	Fitting the model.....	144
4.4.2(c)	Effect of independent variables on the nanoparticle size of ACD_AgNP .....	145

4.4.2(d)	Effect of independent variables on the conjugation efficiency of ACD_AgNP.....	147
4.4.2(e)	Verification of the optimised solution generated by the RSM.....	149
4.4.3	UL_CNP synthesised silver nanoparticles (UL_AgNP) .....	150
4.4.3(a)	Optimisation of UL_AgNP synthesis .....	151
4.4.3(b)	Fitting the model.....	152
4.4.3(c)	Effect of independent variables on the nanoparticle size of UL_AgNP .....	153
4.4.3(d)	Effect of independent variables on the conjugation efficiency of UL_AgNP.....	155
4.4.3(e)	Verification of the optimised solution generated by the RSM.....	156
4.5	Characterisation of AgNP .....	157
4.5.1	Ultraviolet-visible spectroscopy (UV-Vis) .....	157
4.5.2	Attenuated total reflectance-Fourier transform infrared spectroscopy (ATR-FTIR) .....	159
4.5.3	Zeta potential, hydrodynamic size and size distribution .....	161
4.5.4	X-ray diffractometry analysis (XRD) .....	164
4.5.5	Scanning electron microscopy (SEM).....	165
4.5.5(a)	Energy dispersive X-ray analysis (EDX) .....	167
4.5.6	Transmission electron microscopy (TEM).....	168
4.6	Brine shrimp ( <i>Sain vivo</i> ) lethality bioassay .....	169
4.7	Antibacterial activity .....	174
4.7.1	Kirby-Bauer disc diffusion assay .....	174
4.7.2	Broth microdilution assay .....	175
4.7.3	Time-kill kinetics assay.....	177
4.8	Bacterial gene expression study .....	180
4.8.1	Qualitative polymerase chain reaction (PCR).....	180
4.8.2	mRNA expression profile of targeted genes on <i>E. coli</i> .....	182

4.8.3	mRNA expression profile of targeted genes on <i>S. aureus</i> .....	188
<b>CHAPTER 5 CONCLUSION AND FUTURE RECOMMENDATIONS....</b>		<b>193</b>
5.1	Conclusion.....	193
5.2	Research limitation.....	195
5.3	Recommendations for future research.....	195
<b>REFERENCES.....</b>		<b>197</b>
<b>APPENDICES</b>		
<b>LIST OF PUBLICATIONS</b>		

## LIST OF TABLES

		<b>Page</b>
Table 2.1	The pharmacological activities of <i>C. nutans</i> leaf extracts. ....	12
Table 2.2	Advantages and disadvantages of the major approaches in metabolomics. Adapted from Fraga-Corral et al. (2022). ....	23
Table 2.3	Advantages and disadvantages of analytical techniques used in metabolite profiling. Adapted from Fraga-Corral et al. (2022). ....	25
Table 2.4	Antibacterial activities of plant crude polysaccharide/polysaccharide-complex synthesised AgNP .....	44
Table 2.5	Antibiotic classes and their primary targets. Adapted from Peach et al. (2013). ....	53
Table 2.6	An example of experimental matrices for BBD.....	64
Table 3.1	List of chemicals, reagents and kits .....	67
Table 3.2	List of lab equipment and devices.....	68
Table 3.3	Variables and their coded level values used for ALK_AgNP and UL_AgNP for the BBD optimisation.....	79
Table 3.4	Variables and their coded level values used for ACD_AgNP for the BBD optimisation.....	79
Table 3.5	Primers designed for <i>E. coli</i> .....	88
Table 3.6	Primers designed for <i>S. aureus</i> .....	88
Table 4.1	Extraction yield of FT_CNP (%). Data are expressed as mean $\pm$ SD (n=3). ....	100
Table 4.2	A comparison of the optimised/highest average yield and parameters in different extraction methods of CNP (%). Data are expressed as mean $\pm$ SD (n=3). Different lower-case letter(s) show statistically significant differences ( $p < 0.05$ ) between groups according to Tukey's multiple comparison tests.....	104

Table 4.3	A comparison of IC <sub>50</sub> in different extraction methods of CNP. Data are expressed as mean ± SD (n=3). Different lower-case letter(s) show statistically significant differences ( <i>p</i> < 0.05) between groups according to Tukey's multiple comparison tests.....	116
Table 4.4	Putative metabolites in CNP detected by GC-MS analysis. ....	129
Table 4.5	Box-Behnken design matrix with actual and predicted responses of the nanoparticle size ( <i>X</i> <sub>1</sub> ) and conjugation efficiency ( <i>X</i> <sub>2</sub> ). ....	137
Table 4.6	ANOVA results of the BBD model for the particle size ( <i>X</i> <sub>1</sub> ) and conjugation efficiency ( <i>X</i> <sub>2</sub> ). ....	137
Table 4.7	ANOVA results for the linear model of nanoparticle size ( <i>X</i> <sub>1</sub> ) .....	139
Table 4.8	ANOVA results for the quadratic model of conjugation efficiency ( <i>X</i> <sub>2</sub> ) .....	141
Table 4.9	Optimised factors and their predicted and actual responses. ....	142
Table 4.10	Box-Behnken design matrix with actual and predicted responses of the nanoparticle size ( <i>X</i> <sub>1</sub> ) and conjugation efficiency ( <i>X</i> <sub>2</sub> ). ....	144
Table 4.11	ANOVA results of the BBD model for the particle size ( <i>X</i> <sub>1</sub> ) and conjugation efficiency ( <i>X</i> <sub>2</sub> ). ....	145
Table 4.12	ANOVA results for the linear model of nanoparticle size ( <i>X</i> <sub>1</sub> ) .....	146
Table 4.13	ANOVA results for the quadratic model of conjugation efficiency ( <i>X</i> <sub>2</sub> ) .....	148
Table 4.14	Optimised factors and their predicted and actual responses. ....	150
Table 4.15	Box-Behnken design matrix with actual and predicted responses of the nanoparticle size ( <i>X</i> <sub>1</sub> ) and conjugation efficiency ( <i>X</i> <sub>2</sub> ). ....	152
Table 4.16	ANOVA results of the BBD model for the particle size ( <i>X</i> <sub>1</sub> ) and conjugation efficiency ( <i>X</i> <sub>2</sub> ). ....	153
Table 4.17	ANOVA for the reduced linear model nanoparticle size ( <i>X</i> <sub>1</sub> ).....	154
Table 4.18	ANOVA results for the quadratic model of conjugation efficiency ( <i>X</i> <sub>2</sub> ) .....	156
Table 4.19	Optimised factors and their predicted and actual responses. ....	157

Table 4.20	The summary of the average size, PDI and zeta potential of ALK_AgNP, ACD_AgNP and UL_AgNP. Data are represented as mean $\pm$ SD for n=3.....	164
Table 4.21	Kirby-Bauer disc diffusion ZOI of treatment groups against <i>E. coli</i> and <i>S. aureus</i> . These data represent mean $\pm$ SD of n=3. NA symbolises no bacterial activity found. Different lower-case letter(s) show statistically significant differences ( $p < 0.05$ ) between groups according to Tukey's multiple comparison tests. ..	175
Table 4.22	MIC and MBC of treatment groups against <i>E. coli</i> and <i>S. aureus</i> . NA symbolises no bacterial activity found. These data represent mean $\pm$ SD of n=3. Different lower-case letter(s) show statistically significant differences ( $p < 0.05$ ) between groups for MIC and MBC values, respectively, according to Tukey's multiple comparison tests.....	177
Table 4.23	Semi quantitative quantification of band intensity of the gel electrophoresis of <i>gyrA</i> , <i>gyrB</i> , <i>parC</i> , <i>parE</i> , <i>topA</i> , <i>topB</i> and <i>dnaG</i> genes in <i>E. coli</i> and <i>S. aureus</i> genomic DNA with 35 cycles.....	181

## LIST OF FIGURES

	<b>Page</b>
Figure 2.1	<i>Clinacanthus nutans</i> plant. Plant Source: Herb Garden, Animal Research Complex, Advanced Medical and Dental Institute, Universiti Sains Malaysia. .... 11
Figure 2.2	Omics approach and hierarchy. Extracted from Frueh & Burczynski (2020). .... 22
Figure 2.3	Physical, chemical and biological synthesis of NP. Adapted from Bloch et al. (2021). .... 28
Figure 2.4	Mechanism of AgNP green synthesis from plant. Extracted from Nazia Tarannum et al. (2019). .... 34
Figure 2.5	General mechanism of metallic nanoparticles synthesis. Extracted from Devasvaran & Lim (2021). .... 36
Figure 2.6	Sucrose hydrolysis into glucose and fructose, in its open and closed form. Extracted from Agudelo et al. (2018). .... 37
Figure 2.7	Oxidation of glucose in gluconic acid and gluconic acid salt. Extracted from Agudelo et al. (2018). .... 38
Figure 2.8	Proposed AgNP antibacterial mechanism of action. Extracted from Devasvaran & Lim (2021) ..... 48
Figure 2.9	Cell wall of gram-positive and gram-negative bacteria. Extracted from Steward (2019). .... 50
Figure 2.10	Structure and principal function of Topoisomerase II and IV. Adapted from Blondeau (2004). .... 58
Figure 2.11	Structure of ciprofloxacin. Adapted from Sharma et al. (2010) ..... 59
Figure 2.12	Two types of experimental design with three factors. Adapted from E. Ansari & Hughes (2016). .... 63
Figure 2.13	Experimental designs based on the study of all variables in three levels: three-level factorial design for the optimisation of (A) two

	variables, (B) three variables and (C) BBD for the optimisation of three variables. Adapted from Bezerra et al. (2008).....63
Figure 4.1	Effects of (A) solid-liquid ratio; (B) extraction temperature (°C) and (C) extraction time (h) on the extraction yield of HW_CNP (%). Data are expressed as mean ± SD (n=3). Different lower-case letter(s) show statistically significant differences ( $p < 0.05$ ) between groups according to Tukey's multiple comparison tests. ....97
Figure 4.2	Effects of (A) solid-liquid ratio; (B) extraction temperature (°C) and (C) extraction time (min) on the extraction yield of UL_CNP (%). Data are expressed as mean ± SD (n=3). Different lower-case letter(s) show statistically significant differences ( $p < 0.05$ ) between groups according to Tukey's multiple comparison tests. ....99
Figure 4.3	Effects of (A) extraction pH; (B) extraction temperature (°C) and (C) extraction time (h) on the extraction yield of ALK_CNP (%). Data are expressed as mean ± SD (n=3). Different lower-case letter(s) show statistically significant differences ( $p < 0.05$ ) between groups according to Tukey's multiple comparison tests. ..101
Figure 4.4	Effects of (A) citric acid concentration (M), (B) extraction temperature (°C) and (C) extraction time (h) on the extraction yield of ACD_CNP (%). Data are expressed as mean ± SD (n=3). Different lower-case letter(s) show statistically significant differences ( $p < 0.05$ ) between groups according to Tukey's multiple comparison tests.....103
Figure 4.5	A comparison of total carbohydrate content [glucose equivalent (µg/mL)] in different extraction methods of CNP. Data are expressed as mean ± SD (n=3). Different lower-case letter(s) show statistically significant differences ( $p < 0.05$ ) between groups according to Tukey's multiple comparison tests.....105
Figure 4.6	A comparison of total protein content [albumin equivalent (µg/mL)] in different extraction methods of CNP. Data are expressed as mean ± SD (n=3). Different lower-case letter(s) show



	statistically significant differences ( $p < 0.05$ ) between groups according to Tukey's multiple comparison tests.....	107
Figure 4.7	A comparison of total phenolic content [gallic acid equivalent ( $\mu\text{g/mL}$ )] in different extraction methods of CNP. Data are expressed as mean $\pm$ SD ( $n=3$ ). Different lower-case letter(s) show statistically significant differences ( $p < 0.05$ ) between groups according to Tukey's multiple comparison tests.....	109
Figure 4.8	A comparison of total DPPH scavenging activity in different extraction methods of CNP. Data are expressed as mean $\pm$ SD ( $n=3$ ). Different lower-case letter(s) show statistically significant differences ( $p < 0.05$ ) between groups according to Tukey's multiple comparison tests.....	112
Figure 4.9	A comparison of total ABTS scavenging activity in different extraction methods of CNP. Data are expressed as mean $\pm$ SD ( $n=3$ ). Different lower-case letter(s) show statistically significant differences ( $p < 0.05$ ) between groups according to Tukey's multiple comparison tests.....	114
Figure 4.10	A comparison of total phenolic content in different extraction methods of CNP against the $\text{IC}_{50}$ of DPPH and ABTS. Data are expressed as mean $\pm$ SD ( $n=3$ ). .....	115
Figure 4.11	ATR-FTIR spectra of different extraction methods of CNP.....	118
Figure 4.12	The principal component analysis (PCA) of different extraction methods of CNP, using ATR-FTIR represented by (A) PCA score scatter plot and (B) PCA biplot. The data is represented by $n=6$ for each CNP.....	120
Figure 4.13	Partial least square (PLS) of different extraction methods of CNP, using ATR-FTIR represented by (A) PLS score plot, (B) PLS biplot showing the correlation between identified compound with antioxidant activity $X=\text{compounds}$ , $Y=\text{antioxidant activity}$ , (C) PLS biplot showing the correlation of CNP with $Y= \text{antioxidant activity}$ and (D) PLS variable importance in the projection (VIP) values. The VIP values of $> 3.0$ are represented by blue coloured	

	bars, while 2.9 - 0.5 in green and red coloured bars represent < 0.5 VIP values. ....	123
Figure 4.14	Heatmap of the significant top 25 metabolites, including the DPPH and ABTS present in the five CNP. The scale value of 1.5 (maroon) indicated the highest intensity, while the value -1.5 (dark blue) indicated the lowest intensity. ....	124
Figure 4.15	Statistical validation plot of 100 permutations for PLS model of (A) DPPH and (B) ABTS, antioxidant activity in CNP. The R2 (green circles) and Q2 (blue boxes) values from the permuted analysis (bottom left) are significantly lower than the corresponding original values (top right). ....	125
Figure 4.16	GC-MS chromatogram of the HW_CNP. Labelled peaks: <b>1-</b> D-arabinose, <b>2-</b> Tetrahydroxypentanoic acid, <b>3-</b> Mannose, <b>4-</b> Arabinose, <b>5-</b> alpha-D-galactopyranose, <b>6-</b> D-ribose, <b>7-</b> Glucaric acid, <b>8-</b> D-xylose and <b>9-</b> Glucopyranose. The fragment m/z spectra of all compounds were compared to the NIST05 database with a similarity index above 90%. ....	127
Figure 4.17	GC-MS chromatogram of the ALK_CNP. Labelled peaks: <b>1-</b> Butanedioic acid, <b>2-</b> D-arabinose, <b>3-</b> Arabinose, <b>4-</b> D-xylopyranose, <b>5-</b> Arabinopyranose, <b>6-</b> Pentaric acid, <b>7-</b> D-galactose, <b>8-</b> Glucaric acid and <b>9-</b> Glucopyranose. The fragment m/z spectra of all compounds were compared to the NIST05 database with a similarity index above 90%. ....	127
Figure 4.18	GC-MS chromatogram of the UL_CNP. Labelled peaks: <b>1-</b> D-arabinose, <b>2-</b> Arabinose, <b>3-</b> Pentaric acid, <b>4-</b> alpha-D-xylopyranose, <b>5-</b> alpha-D-galactopyranose, <b>6-</b> D-galactose, <b>7-</b> Glucaric acid, <b>8-</b> D-xylose and <b>9-</b> Glucopyranose. The fragment m/z spectra of all compounds were compared to the NIST05 database with a similarity index above 90%. ....	128
Figure 4.19	GC-MS chromatogram of the FT_CNP. Labelled peaks: <b>1-</b> D-arabinose, <b>2-</b> Arabinose, <b>3-</b> D-xylopyranose, <b>4-</b> Arabinopyranose, <b>5-</b> Pentaric acid, <b>6-</b> alpha-D-xylopyranose, <b>7-</b> alpha-D-	

	galactopyranose, <b>8</b> - D-galactose, <b>9</b> - Glucaric acid, <b>10</b> - D-xylose and <b>12</b> - Glucopyranose. The fragment m/z spectra of all compounds were compared to the NIST05 database with a similarity index above 90%.....	128
Figure 4.20	GC-MS chromatogram of the ACD_CNP. Labelled peaks: <b>1</b> - D-arabinose, <b>2</b> - Arabinose, <b>3</b> - alpha-D-galactopyranose, <b>4</b> - D-galactose, <b>5</b> - D-xylose, and <b>6</b> - Galacturonic acid. The fragment m/z spectra of all compounds were compared to the NIST05 database with a similarity index above 90%.....	129
Figure 4.21	The principal component analysis (PCA) of different extraction methods of CNP, using GC-MS represented by (A) PCA score scatter plot and (B) PCA biplot. The data is represented by n=6 for each CNP.....	132
Figure 4.22	Heatmap of the 17 different monosaccharides/ sugar acids found in the five CNP. The scale value of 1.5 (maroon) indicated the highest intensity, while the value -1.5 (dark blue) indicated the lowest intensity. ....	133
Figure 4.23	UV-Vis absorption spectra of different (A) concentration (mg/mL), (B) ratio and (C) time (min) of silver nanoparticles synthesised using ALK_CNP as a stabilising agent. The excitation of surface plasmon vibrations of silver nanoparticles appears in the range of 380 - 480 nm. ....	135
Figure 4.24	3D-response surface plot of the synthesised ALK_AgNP on the characteristic features of the size (nm) effect (A) as a function of concentration (mg/mL) and ratio; (B) as a function of time and ratio and (C) as a function of concentration (mg/mL) and time. ....	139
Figure 4.25	3D-response surface plot of the synthesised ALK_AgNP on the characteristic features of the conjugation efficiency (%) effect (A) as a function of concentration (mg/mL) and ratio; (B) as a function of time and ratio and (C) as a function of concentration (mg/mL) and time.....	141

Figure 4.26	UV-Vis absorption spectra of different (A) concentration (mg/mL), (B) ratio and (C) time (min) of silver nanoparticles synthesized using ACD_CNP as a stabilising agent. The excitation of surface plasmon vibrations of silver nanoparticles appears in the range of 380 - 480 nm. ....	143
Figure 4.27	3D-response surface plot of the synthesised ACD_AgNP on the characteristic features of the size (nm) effect (A) as a function of concentration (mg/mL) and ratio; (B) as a function of time and ratio and (C) as a function of concentration (mg/mL) and time. ....	147
Figure 4.28	3D-response surface plot of the synthesised ACD_AgNP on the characteristic features of the conjugation efficiency (%) effect (A) as a function of concentration (mg/mL) and ratio; (B) as a function of time and ratio and (C) as a function of concentration (mg/mL) and time. ....	149
Figure 4.29	UV-Vis absorption spectra of different (A) concentration (mg/mL), (B) ratio and (C) time (min) of silver nanoparticles synthesised using UL_CNP as a stabilising agent. The excitation of surface plasmon vibrations of silver nanoparticles appears in the range of 380 - 480 nm. ....	151
Figure 4.30	3D-response surface plot of the synthesised UL_AgNP on the characteristic features of the size (nm) effect (A) as a function of concentration (mg/mL) and ratio; (B) as a function of time and ratio and (C) as a function of concentration (mg/mL) and time. ....	154
Figure 4.31	3D-response surface plot of the synthesised UL_AgNP on the characteristic features of the conjugation efficiency (%) effect (A) as a function of concentration (mg/mL) and ratio; (B) as a function of time and ratio and (C) as a function of concentration (mg/mL) and time. ....	156
Figure 4.32	UV-Vis absorption spectra of AgNP (ALK_AgNP, ACD_AgNP and UL_AgNP) and controls (ALK_CNP, ACD_CNP, UL_CNP and AgNO <sub>3</sub> ). The excitation of surface plasmon vibrations of the three AgNP appears in the range of silver nanoparticles (380 - 480	

	nm), while the controls do not appear to have any excitation in the AgNP plasmon vibrations. ....	159
Figure 4.33	ATR-FTIR spectra of ALK_CNP, ALK_AgNP, ACD_CNP, ACD_AgNP, UL_CNP and UL_AgNP. ....	161
Figure 4.34	Particles size analysis of the biosynthesised AgNP represented by; (A) ALK_AgNP, (C) ACD_AgNP and (E) UL_AgNP, while zeta potential represented by; (B) ALK_AgNP, (D) ACD_AgNP and (F) UL_AgNP. The data are represented by the average of three independent readings.....	163
Figure 4.35	XRD graphs of AgNP represented by; (A) Standard_AgNP, (B) ALK_AgNP and (C) UL_AgNP. ....	165
Figure 4.36	SEM images of AgNP represented by; (A) Standard_AgNP, (C) ALK_AgNP and (E) UL_AgNP. The particle size distributions are shown in the histograms, represented by; (B) Standard_AgNP, (D) ALK_AgNP and (F) UL_AgNP. The data are expressed as mean $\pm$ SD for 100 nanoparticles. ....	166
Figure 4.37	EDX spectrum of AgNP represented by; (A) Standard_AgNP, (B) ALK_AgNP and (C) UL_AgNP. ....	167
Figure 4.38	TEM image of spherical silver nanoparticles represented by; (A) Standard AgNP, (C) ALK_AgNP and (E) UL_AgNP. The particle size distributions are shown in the histograms, represented by; (B) Standard AgNP, (D) ALK_AgNP and (F) UL_AgNP. The data are expressed as mean $\pm$ SD for 100 nanoparticles.....	169
Figure 4.39	Effects of various concentrations of (A) positive control, (B) Standard_AgNP, (C) ALK_CNP, (D) ALK_AgNP, (E) UL_CNP and (F) UL_AgNP on the mortality percentage (%) of brine shrimp nauplii ( <i>Artemia franciscana</i> ) after 4, 8, 12 and 24 h of treatment. Data are expressed as mean $\pm$ SD of 15 shrimps for each concentration. After 24 h, images were taken to identify any morphological changes (Appendix E).....	173

Figure 4.40	Kirby-Bauer disc diffusion ZOI of (A) <i>E. coli</i> and (B) <i>S. aureus</i> . Labelled groups: <b>1-</b> ALK_AgNP (1 mg/mL), <b>2-</b> ALK_CNP (1 mg/mL), <b>3-</b> Standard_AgNP (1 mg/mL), <b>4-</b> Ciprofloxacin (100 µg/mL) and <b>5-</b> Negative control (distilled water). ....	175
Figure 4.41	Time-kill curve against (A) <i>E. coli</i> and (B) <i>S. aureus</i> treated with the respective MBC concentration of ALK_AgNP at 0.5, 3, 6 and 12 h treatment periods. These data represent mean ± SD of n=3. ...	179
Figure 4.42	Images of time-kill kinetics assay of ALK_AgNP exposed to <i>E. coli</i> and <i>S. aureus</i> at the respective MBC concentration for 0.5, 3, 6 and 12 h. These images represent n=3 for each treatment time. ...	180
Figure 4.43	Agarose gel electrophoresis of PCR product for <i>gyrA</i> , <i>gyrB</i> , <i>parC</i> , <i>parE</i> , <i>topA</i> , <i>topB</i> and <i>dnaG</i> genes in (A) <i>E. coli</i> and (B) <i>S. aureus</i> genomic DNA. Lane M: DNA molecular weight marker (100bp ladder). ....	181
Figure 4.44	mRNA expression of genes in <i>E. coli</i> . RT-qPCR results showing the relative mRNA expression level of; (A) <i>gyrA</i> , (B) <i>gyrB</i> , (C) <i>parC</i> , (D) <i>parE</i> , (E) <i>topA</i> and (F) <i>topB</i> genes. Data are expressed as mean ± SD (n=3). Dash line indicate untreated group/negative control (1-fold expression). Different lower-case letter(s) show statistically significant differences ( $p < 0.05$ ) between groups according to Tukey's multiple comparison tests.....	187
Figure 4.45	mRNA expression of genes in <i>S. aureus</i> . RT-qPCR results showing the relative mRNA expression level of; (A) <i>gyrA</i> , (B) <i>gyrB</i> , (C) <i>parC</i> , (D) <i>parE</i> , (E) <i>topA</i> and (F) <i>topB</i> genes. Data are expressed as mean ± SD (n=3). Dash line indicate untreated group (1-fold expression). Different lower-case letter(s) show statistically significant differences ( $p < 0.05$ ) between groups according to Tukey's multiple comparison tests.....	192

## LIST OF SYMBOLS

°	Degree
°C	Degree Celsius
=	Equals
$\gamma$	Gamma
$\geq$	Greater-than or equal to
$\lambda$	Lambda
$\leq$	Less-than or equal to
$\mu$	Micro
%	Percentage
-	Minus
+	Plus
$\pm$	Plus-minus

## LIST OF ABBREVIATIONS

ABTS	2,2'-azino-bis(3-ethylbenzothiazoline-6-sulfonic acid)
ACD_AgNP	ACD_CNP synthesised silver nanoparticles
ACD_CNP	Acid extraction of <i>C. nutans</i> leaf crude polysaccharide
Ag	Silver
Ag <sup>+</sup>	Silver ion
AgNO <sub>3</sub>	Silver nitrate
AgNP	Silver nanoparticles
ALK_AgNP	ALK_CNP synthesised silver nanoparticles
ALK_CNP	Alkaline extraction of <i>C. nutans</i> leaf crude polysaccharide
ANOVA	Analysis of variance
ATCC	American Type Cell Culture Collection
ATR-FTIR	Attenuated total reflectance (ATR)-Fourier transform infrared spectroscopy
BBD	Box-Behnken design
<i>C. nutans</i>	<i>Clinacanthus nutans</i>
CLSI	Clinical and Laboratory Standards Institute
CNP	<i>C. nutans</i> leaf crude polysaccharide
DLS	Dynamic light scattering
DNA	Deoxyribonucleic acid
DPPH	2,2-diphenyl-1-picryl-hydrazyl-hydrate
<i>E. coli</i>	<i>Escherichia coli</i>
EDX	Energy dispersive X-ray analysis
FT_CNP	Freeze-thaw extraction of <i>C. nutans</i> leaf crude polysaccharide
FTIR	Fourier transform infrared spectroscopy
GC-MS	Gas chromatography–mass spectrometry



h	Hour
HW_CNP	Hot water extraction of <i>C. nutans</i> leaf crude polysaccharide
IC <sub>50</sub>	Half-maximal inhibitory concentration
JCPDS	Joint Committee on Powder Diffraction Standard
LC <sub>50</sub>	Lethal concentration 50
M	Molar
MBC	Minimum bactericidal concentration
mg/mL	Milligram per milliliter
MIC	Minimum inhibitory concentration
min	Minute
mm	Millimeter
mM	Milli mol
MOA	Mechanism of action
mRNA	Messenger RNA
MS	Mass spectrometry
MVDA	Multivariate data analysis
nm	Nanometer
PCA	Principal component analysis
PC-DFA	Principal components-discriminant function analysis
PCR	Polymerase chain reaction
PDI	Polydispersity index
pH	Potential of hydrogen
PLS	Partial least squares
R <sup>2</sup>	Correlation coefficient
RNA	Ribonucleic acid
ROS	Reactive oxygen species
RSM	Response surface method

s	Second
<i>S. aureus</i>	<i>Staphylococcus aureus</i>
SD	Standard deviation
SEM	Scanning electron microscopy
SPR	Surface plasmon resonance
Standard_AgNP	Silver nanoparticles from Sigma-Aldrich
TEM	Transmission electron microscopy
TPC	Total phenolic content
UL_AgNP	UL_CNP synthesised silver nanoparticles
UL_CNP	Ultrasound-assisted extraction of <i>C. nutans</i> leaf crude polysaccharide
UV-Vis	Ultraviolet-visible spectroscopy
VIP	Variable importance in projection
XRD	X-ray diffractometry analysis
ZOI	Zone of inhibition
µg/mL	Micro gram per milliliter
µL	Micro liter

## LIST OF APPENDICES

Appendix A	GC-MS random sequence generated from random.org
Appendix B	Standard curves of CNP content analysis
Appendix C	Standard curves of CNP antioxidant analysis
Appendix D	Metabolomics (ATR-FTIR) VIP values of > 3.0
Appendix E	Brine shrimp images after 24 h treatment

**SINTESIS HIJAU NANOPARTIKEL PERAK DARI POLISAKARIDA  
LARUT DALAM AIR DARI DAUN *CLINACANTHUS NUTANS*:  
PENGEKSTRAKAN, PERINCIAN, PENGOPTIMUMAN DAN KAJIAN  
ANTIBAKTERIA**

**ABSTRAK**

*C. nutans* telah mendapat banyak perhatian oleh penyelidik kerana sifat farmakoterapeutiknya. Walau bagaimanapun, kaedah pengekstrakan polisakarida mentah *C. nutans* (CNP), sintesis nanopartikel perak (AgNP) daripada CNP dan sifat antibakteria serta, sebagai perencat sintesis DNA belum dikaji. Oleh itu, penyelidikan ini bertujuan untuk menggunakan kaedah hijau (CNP) untuk menghasilkan AgNP dan menilai potensi penggunaannya sebagai agen antibakteria. CNP diekstrak menggunakan lima kaedah iaitu air panas (HW\_CNP), ultrabunyi (UL\_CNP), beku-cair (FT\_CNP), alkali (ALK\_CNP) dan asid (ACD\_CNP). Kelima-lima CNP telah dioptimumkan, dicirikan dan komposisinya telah dianalisa. Tiga CNP kemudiannya dipilih untuk mensintesis ACD\_AgNP, ALK\_AgNP, dan UL\_AgNP masing-masing, di mana ALK\_AgNP dan UL\_AgNP dipilih berdasarkan keadaan sintesisnya dan ketoksikannya dalam udang pekasin dikuantitasi. Di sini, potensi sebagai agen antibakteria serta mekanisme tindakan perencatan sintesis DNA antibakteria ALK\_AgNP dikaji. Keputusan CNP menunjukkan bahawa ACD\_CNP dan FT\_CNP memperoleh hasil pengekstrakan tertinggi dan terendah masing-masing pada  $14.85 \pm 0.25\%$  dan  $4.16 \pm 0.13\%$ . Manakala kandungan karbohidrat dan protein tertinggi dilaporkan oleh HW\_CNP [ $287.72 \pm 16.14$  setara glukosa ( $\mu\text{g/mL}$ )] dan UL\_CNP [ $19.09 \pm 0.95$  setara albumin ( $\mu\text{g/mL}$ )]. FT\_CNP mempamerkan kandungan fenolik tertinggi [ $418.49 \pm 1.91$  setara asid galik ( $\mu\text{g/mL}$ )] dengan  $\text{IC}_{50}$  keantioksidan terendah

pada  $380.37 \pm 53.20 \mu\text{g/mL}$  (DPPH) dan  $186.43 \pm 2.93 \mu\text{g/mL}$  (ABTS). Analisis ATR-FTIR dan GC-MS mengesahkan pengekstrakan CNP, manakala metabolomik menggambarkan pemisahan CNP dalam tiga kelompok. Dari sini, keadaan sintesis optimum ACD\_AgNP, ALK\_AgNP, dan UL\_AgNP berbeza-beza, namun; ALK\_AgNP mempunyai saiz hidrodinamik terendah ( $66.74 \pm 1.43 \text{ nm}$ ) dan kestabilan koloid tertinggi ( $-30.63 \pm 0.86 \text{ mV}$ ). UV-Vis dan ATR-FTIR mengesahkan pembentukan AgNP masing-masing. SEM memperlihatkan struktur sfera, manakala TEM mengesahkan saiz AgNP tersebut (ALK\_AgNP pada  $7.48 \pm 2.88 \text{ nm}$  dan UL\_AgNP pada  $5.21 \pm 1.92 \text{ nm}$ ). Dalam cerakin udang pekasin, peratus kematian akibat ALK\_AgNP adalah lebih rendah daripada UL\_AgNP selepas 24 jam. Dalam *E. coli* dan *S. aureus* pula, ALK\_AgNP membentuk zon perencatan sebanyak  $11.33 \pm 0.58$  dan  $12.00 \pm 1.00 \text{ mm}$ , masing-masing. MIC dan MBC ALK\_AgNP adalah dua-kali ganda lebih rendah dalam *E. coli* berbanding *S. aureus*. ALK\_AgNP juga memaparkan perencatan sintesis DNA dalam kedua-dua *E. coli* dan *S. aureus*, manakala Standard\_AgNP hanya memaparkannya di *S. aureus*. Oleh itu, ALK\_CNP yang diekstrak dalam penyelidikan ini terbukti sebagai agen pengurangan yang berjaya untuk mensintesis ALK\_AgNP dengan saiz yang kecil dan telah menunjukkan ketoksikan yang rendah dalam *in vivo*, serta ciri yang menjanjikan sebagai agen antibakteria yang berkesan dengan sifat perencatan sintesis DNA bakteria.

**GREEN SYNTHESIS OF SILVER NANOPARTICLES FROM WATER-SOLUBLE POLYSACCHARIDES OF *CLINACANTHUS NUTANS* LEAF: EXTRACTION, CHARACTERISATION, OPTIMISATION AND ANTIBACTERIAL STUDIES**

**ABSTRACT**

*C. nutans* has gained much attention by researchers due to its pharmacotherapeutic properties. However, the extraction method of *C. nutans* leaf crude polysaccharide (CNP), CNP synthesising silver nanoparticles (AgNP) and the subsequent antibacterial properties as a DNA synthesis inhibitor, has not been studied. Hence, this research aims to employ a green synthetic method to produce AgNP and assess its potential application as an antibacterial agent. Five extraction methods of CNP were employed, namely hot water (HW\_CNP), ultrasound-assisted (UL\_CNP), freeze-thaw (FT\_CNP), alkaline (ALK\_CNP) and acid (ACD\_CNP). All five CNP were optimised and characterised, and their compositions were analysed. Three CNP were then selected to synthesise ACD\_AgNP, ALK\_AgNP, and UL\_AgNP, respectively, where ALK\_AgNP and UL\_AgNP were optimally selected based on their synthesis conditions and their toxicity in brine shrimp was quantified. The antibacterial and potential DNA synthesis inhibition mechanism of action (MOA) of ALK\_AgNP was further quantified. The results of CNP showed that ACD\_CNP and FT\_CNP obtained the highest and lowest extraction yield at  $14.85 \pm 0.25\%$  and  $4.16 \pm 0.13\%$ , respectively. While the highest carbohydrate and protein content were reported by HW\_CNP [ $287.72 \pm 16.14$  glucose equivalent ( $\mu\text{g/mL}$ )] and UL\_CNP [ $19.09 \pm 0.95$  albumin equivalent ( $\mu\text{g/mL}$ )], respectively. FT\_CNP exhibited the highest phenolic content [ $418.49 \pm 1.91$  gallic acid equivalent ( $\mu\text{g/mL}$ )] and the

antioxidant IC<sub>50</sub> at 380.37 ± 53.20 µg/mL (DPPH) and 186.43 ± 2.93 µg/mL (ABTS). The ATR-FTIR functional groups and GC-MS metabolites confirmed the successful extraction of CNP, while metabolomics illustrated the discrimination in three clusters. From here, the optimisation of the synthesis condition of ACD\_AgNP, ALK\_AgNP, and UL\_AgNP varied. ALK\_AgNP reported the smallest hydrodynamic size (66.74 ± 1.43 nm) and highest colloidal stability (-30.63 ± 0.86 mV). The UV-Vis and ATR-FTIR confirmed the formation of the AgNP. The SEM revealed spherical structures, while TEM confirmed the size of AgNP (ALK\_AgNP at 7.48 ± 2.88 nm and UL\_AgNP at 5.21 ± 1.92 nm). In the brine shrimp assay, ALK\_AgNP reported a much lower mortality percentage at 24 h compared to UL\_AgNP. In *E. coli* and *S. aureus*, ALK\_AgNP formed inhibition zones of 11.33 ± 0.58 and 12.00 ± 1.00 mm, respectively. The MIC and MBC were two-fold lower in *E. coli* compared to *S. aureus*. ALK\_AgNP exhibited DNA synthesis inhibition in both *E. coli* and *S. aureus*, while Standard\_AgNP only in *S. aureus*. Thus, the ALK\_CNP extracted in this research proved to be a successful reducing agent to synthesise ALK\_AgNP with a small size and had demonstrated low toxicity in vivo, as well as promising features as an effective antibacterial agent with bacterial DNA synthesis inhibition properties.

# CHAPTER 1

## INTRODUCTION

This chapter introduces the current research topic in a general manner and is divided into six sections. Section 1.1 provides the research background, followed by Section 1.2, which addresses the problem statements. Sections 1.3 and 1.4 address the research hypothesis and research questions, respectively. While Section 1.5 states the research aim and objectives. Section 1.6 provides information on the significance of this study.

### 1.1 Research background

*Clinacanthus nutans* (*C. nutans*) is a perennial plant found in various ASEAN countries, such as Thailand, Indonesia, Malaysia, and Vietnam. It is known locally as Belalai Gajah in Malay and Sabah Snake Grass in English (Arullappan et al., 2014; Teoh, 2021). This plant has been used as a folk medicine in Southeast Asia for many years and has gained widespread attention by researchers due to its medicinal properties. Aside from helping treat various diseases, its natural phytochemical constituents can also help maintain a healthy lifestyle (Teoh, 2021). Crude polysaccharides are polysaccharides which contain small/negligible amounts of protein and phenolic compounds (Ross et al., 2015). Naturally, polysaccharides rarely exist on their own but rather exist as a conjugate with other components which act as a whole in isolation (Chen et al., 2008). A study on tea leaf polysaccharides suggested that in the presence of polyphenols, the reducing ability and DPPH radical scavenging ability were enhanced. The findings suggested that the polyphenols triggered a synergistic elevation in the antioxidant activity (Wang et al., 2013).



Metallic nanoparticles, especially silver nanoparticles (AgNP), have gained much attention as they possess multiple pharmacological activities, including antibacterial, antifungal, anticancer, anti-inflammatory and wound healing properties (Asghar et al., 2018; Wongpreecha et al., 2018; Jacob et al., 2019). Compared to the conventional AgNP, biological/green synthesised AgNP has higher stability, better solubility, and higher yielding properties (Gurunathan et al., 2015). The crude polysaccharide method of green synthesis for AgNP is a method where AgNP are synthesised in a solution of crude polysaccharides and silver nitrate ( $\text{AgNO}_3$ ). Aside from reducing the metal salts, the crude polysaccharide can also act as an in-situ stabilising and capping agent. The capping ability can also reduce toxicity and prevent the aggregation of the AgNP (Roy et al., 2019). Besides, there is no addition of any other chemicals, and crude polysaccharides are completely safe (Nag et al., 2022; Nkhabindze et al., 2022).

The use of microwave-assisted methods for the production of green nanocomposites and nanoparticles has been regarded as a promising green strategy (Kumar et al., 2020). The advantages of using microwaves for the production of green nanomaterials include; reduced energy consumption and shorter reaction times (Torrás & Roig, 2020). Moreover, the microwave-assisted method is known to heat the mixture homogeneously, allowing for the reliable nucleation and uniform size distribution of nanoparticles (Kumar et al., 2020). Microwave heating is a better method for producing smaller sizes of nanostructures due to its higher degree of crystallisation, keeping the agglomeration of the particles in check (Torrás & Roig, 2020). Besides, the synthesis parameters can be altered to acquire the desired nanoparticle properties; for instance, the concentration of certain solvents, precursors,

and temperature can be used to control the size and morphologies of metallic nanoparticles (Kumar et al., 2021).

Silver has been shown to possess antimicrobial properties (Bindhu et al., 2014; Manikandan et al., 2015). Even though the exact mechanism of AgNP antibacterial effects has not been completely explained, several mechanisms have been proposed. For instance, releasing silver ions from AgNP can be considered as the mechanism of killing microbes (Bapat et al., 2018). Silver ions can adhere to the cell wall and cytoplasmic membrane owing to electrostatic attraction and affinity to sulphur proteins, and this leads to the disruption of the bacterial envelope (Khorrami et al., 2018). After the uptake of free silver ions into cells, respiratory enzymes can be deactivated by interrupting adenosine triphosphate production, and reactive oxygen species (ROS) will be generated (Ramkumar et al., 2017). ROS can be a principal agent in the provocation of cell membrane disruption and deoxyribonucleic acid (DNA) modification. Moreover, silver ions can inhibit protein synthesis by denaturing ribosomes in the cytoplasm (Durán et al., 2016).

Antibiotics are drugs that are used to treat bacterial infections. They can inhibit growth or kill bacteria (Kourkouta & Plati, 2018). Antibiotics are categorised based on their nature and their chemical structure or based on their mechanism of action. The 4 main groups of antibiotics based on their mechanism of action are: cell wall synthesis inhibitors, protein synthesis inhibitors, nucleic acid synthesis inhibitors, and metabolic activity inhibitors (Verma et al., 2022). Fluoroquinolones are a class of antibiotics known to inhibit two enzymes (DNA topoisomerases) involved in bacterial DNA synthesis. These enzymes are required for the replication of bacterial DNA, while in human cells, these enzymes function as homodimers. Due to this difference, the clinically-relevant quinolones can discriminate between the human and bacterial type

II topoisomerases (Aldred et al., 2014; Naeem et al., 2016). This enables fluoroquinolones to be both bactericidal and target-specific (Hooper & Jacoby, 2016).

The basic mechanism of action is that the quinolones interact with two enzymes, namely topoisomerase II and topoisomerase IV, in the bacterial cell. Topoisomerase II expresses the DNA gyrase gene, which is composed of *gyrA* and *gyrB* subunits, while topoisomerase IV is composed of two subunits as well, which are *parC* and *parE*. There are another two enzymes, namely topoisomerase I and III, which are also present in bacteria cells but are not the direct targets of quinolones. Nevertheless, topoisomerase I (encodes *topA* gene) does have a role that complements topoisomerase II, which resists the activity of DNA gyrase by preventing and removing negative supercoils from circular DNA (Sutormin et al., 2019; Villain et al., 2021). While topoisomerase III (encodes *topB* gene) is known to play a key role in the stabilisation of the bacterial genome (Yan et al., 2019).

To evaluate the association of all the factors listed above, in this study, five extraction methods of *C. nutans* leaf crude polysaccharide (CNP) was optimised and characterised in terms of their physicochemical properties and then quantified. Three CNP were selected to synthesise AgNP, which was optimised by response surface method (RSM) to obtain the smallest nanoparticle size, with the highest conjugation efficiency. The toxicity of the AgNP was evaluated (in vivo), and the safest CNP-synthesised AgNP was chosen for testing of the antibacterial activity and antibacterial DNA synthesis mechanism. The outcomes of this project would provide knowledge and evidence for the association of crude polysaccharide extraction methods and their effect on the synthesised AgNP properties. This could potentially provide new tools for designing new antibacterial agents as a safer alternative treatment that would promote human health and well-being.

## 1.2 Problem statements

Over the years, *C. nutans* has attracted widespread attention due to its proven medicinal properties in treating snake bites, viral infections, inflammatory diseases as well as some cancers (Kamarudin et al., 2017; Chia et al., 2021; Mohamed et al., 2022). However, the water-soluble crude polysaccharides from this plant have not been studied. Crude polysaccharides have recently gained interest due to their notable antioxidant activity (Cheng & Huang, 2018; Hamed et al., 2020; Huo et al., 2022). Besides, different extraction methods would possibly extract different bioactive crude polysaccharides. Therefore, this study evaluated the compositions of the various extracts of crude polysaccharides from the *C. nutans* leaf.

Apart from that, the understanding of the formation/synthesis of silver nanoparticles (AgNP) utilising crude polysaccharides as a reducing, stabilising and capping agent is still limited. This green synthesis of AgNP using crude plant polysaccharides has numerous advantages, including cost-effectiveness, environmentally-friendly and non-toxic (Nag et al., 2022; Nkhabindze et al., 2022). However, the green synthesised method used for AgNP is also an essential aspect of increasing the pharmacological effect. Therefore, a more recent technique of synthesis, utilising the microwave convection method, was employed to obtain uniform-size distributed AgNP with reduced energy consumption and shorter reaction times (Anjana et al., 2021; Kumar et al., 2020). Thus, this research optimised the synthesis of AgNP from *C. nutans* leaf crude polysaccharides (CNP) via the microwave-assisted method.

Moreover, commercially available and green-synthesised AgNP has always been regarded as a potent antibacterial agent against both gram-positive and gram-negative bacteria (Wongpreecha et al., 2018; Roberto Vazquez-Muñoz et al., 2020;

Urnukhsaikhan et al., 2021). However, until today, there is still a lack of research investigating the antibacterial mechanism of action (MOA) of AgNP. So far, research has identified that AgNP attaches and penetrates the bacterial cell wall, leading to silver ion leakage into the cytosol and causing cell death (Xu et al., 2019). Another possible mechanism proposed was that the influx of AgNP possibly causes an increase in oxidative stress, leading to bacterial protein and DNA damage; and the disruption of the signal transduction pathways in bacteria, potentially inducing bacterial cell apoptosis (Durán et al., 2016; M. Chen et al., 2019). Therefore, this research aimed to investigate the MOA of the CNP-synthesised AgNP by focusing on the bacterial DNA synthesis inhibition by quantifying the mRNA expression of *gyrA*, *gyrB*, *parC*, *parE*, *topA*, and *topB* genes.

### 1.3 Research hypothesis

- i. Different extraction methods of CNP would produce extracts that possess different characteristic features.
- ii. The selected CNP could act as reducing, stabilising and capping agents to synthesise/optimize AgNP.
- iii. The selected CNP synthesised AgNP could be non-toxic against brine shrimp.
- iv. The selected CNP synthesised AgNP may exhibit antibacterial activity against *Escherichia coli* (*E. coli*) and *Staphylococcus aureus* (*S. aureus*).
- v. The antibacterial mechanism exhibited by the selected CNP synthesised AgNP against *E. coli* and *S. aureus* could be by inhibiting the synthesis of bacterial DNA.

## **1.4 Research questions**

- i. Do CNP produced from different extraction methods possess different characteristic features?
- ii. Could the selected CNP acts as reducing, stabilising and capping agents to synthesise/optimize AgNP?
- iii. What is the toxicity level of the selected CNP-synthesised AgNP in brine shrimp?
- iv. Does the selected CNP-synthesised AgNP have antibacterial activity against *E. coli* and *S. aureus*?
- v. Does the selected CNP-synthesised AgNP act as a DNA synthesis inhibitor against *E. coli* and *S. aureus*?

## **1.5 Research aim and objectives**

This research aims to employ a green method for the production of AgNP using CNP and assess the potential application of this nanoparticle as an antibacterial agent.

### **1.5.1 Objectives**

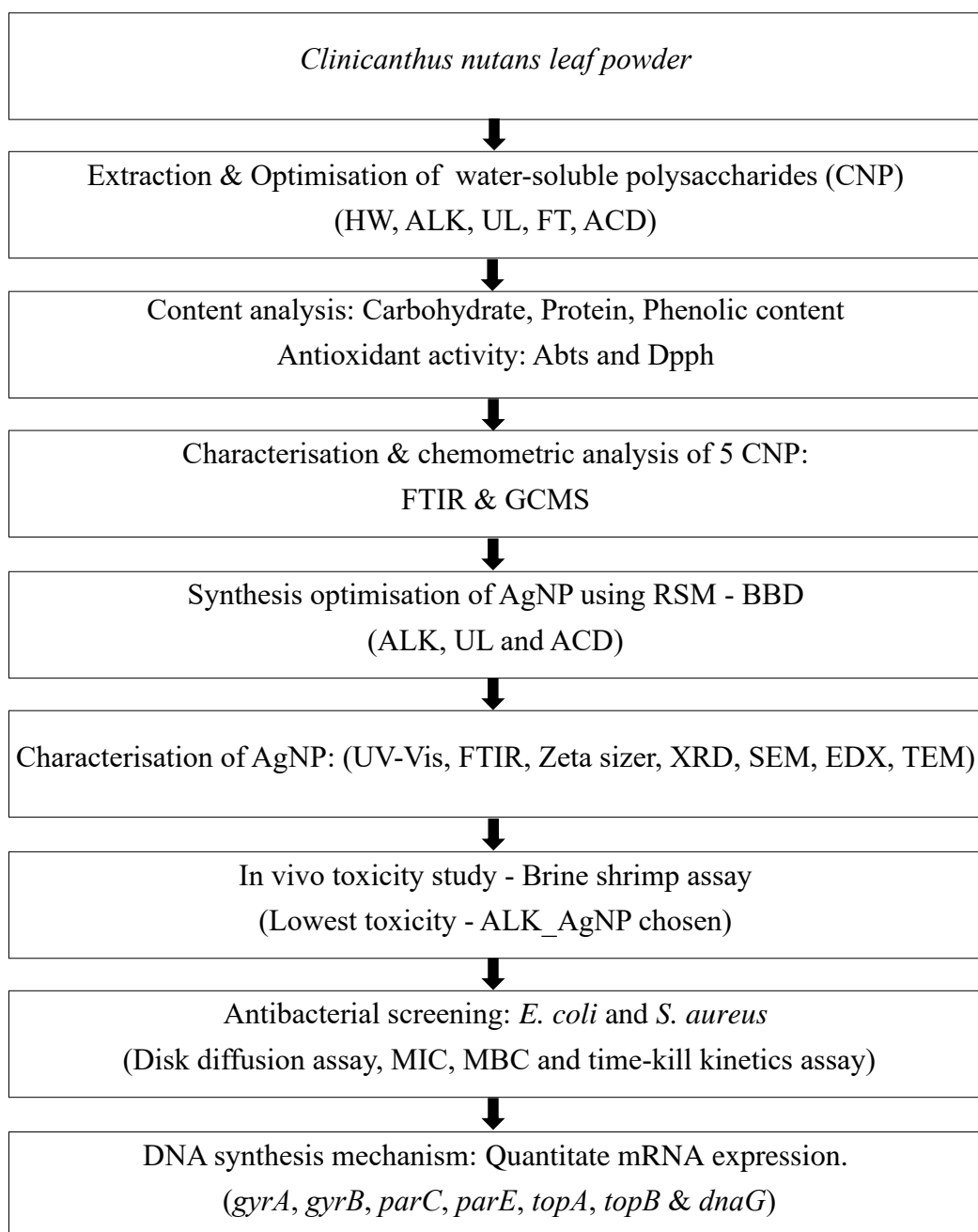
- i. To extract, optimise, characterise and evaluate the composition of five different CNP obtained from different extraction methods.
- ii. To synthesise, optimise and characterise AgNP derived from three selected CNP using the microwave-assisted method.
- iii. To determine the in vivo toxicity exhibited by the selected CNP synthesised AgNP using brine shrimp assay.

- iv. To investigate the antibacterial activity exhibited by the selected CNP synthesised AgNP against *E. coli* and *S. aureus*.
- v. To investigate the bacterial DNA synthesis mechanism by quantifying the targeted gene mRNA expression upon treatment with the selected CNP synthesised AgNP in *E. coli* and *S. aureus*.

## **1.6 Significance of the study**

This project will provide knowledge on the different extraction methods of CNP and their characteristics, as well as the relationship between the CNP-synthesised AgNP physicochemical properties and their toxicity, enabling the production of more efficient AgNP compared to chemically synthesised nanoparticles. Besides, this study also elucidates a novel antibacterial mechanism of the selected CNP synthesised AgNP in relation to the bacterial DNA synthesis genes. This may contribute to the development of a new antimicrobial product utilising plant-mediated green synthesis.

## 1.7 Flow chart of the study





## CHAPTER 2

### LITERATURE REVIEW

This chapter describes the literature review conducted to gain an understanding of the existing research and debates relevant to this research project. Section 2.1 summarises the *Clinacanthus nutans* (*C. nutans*) phytochemical compounds and pharmacological activities. Section 2.2 details about carbohydrates and their antioxidant activity. Meanwhile, Section 2.3 reviews the definition and uses of metabolomics; while Section 2.4 reviews silver nanoparticles, their synthesis mechanism, characterisation techniques and their antibacterial mechanism of action. Section 2.5 reviews the brine shrimp assay, while Section 2.6 details the general topic of gram-positive and gram-negative bacteria. Next, Section 2.7 reviews the classes of antibiotics, specifically the fluoroquinolone class of antibiotics and Section 2.8 reviews the univariate and multivariate data analyses used in this research.

#### 2.1 *Clinacanthus nutans* (*C. nutans*)

*Clinacanthus nutans* is a perennial plant that can be found in various Southeast Asian countries, such as Thailand, Indonesia, Malaysia, and Vietnam. It is locally known as Belalai Gajah in Malay and Sabah Snake Grass in English (Figure 2.1) (Arullappan et al., 2014; Teoh, 2021). In Thailand and Malaysia, it is believed that *C. nutans* can cure snake bites, viral infections, and some cancers, including breast, colon, stomach, lung, and liver cancer (Kunsorn et al., 2013; Kamarudin et al., 2017).

*C. nutans* has also been used to treat various illness such as fever, diabetes, and gastrointestinal diseases (Shim et al., 2013). Its fresh leaves can be used alone or with other herbs for general well-being (Aslam et al., 2015). In Thailand, the leaves were commonly applied to treat insect bites, skin irritations and lesions caused by certain

viruses (Varicella zoster virus and Herpes simplex virus) (Sakdarat et al., 2019). Its phenolic compounds have antioxidant properties that can help cancer patients (Teoh, 2021). In Malaysia, some cancer patients claimed that they were able to recover after drinking a decoction made with *C. nutans* leaves; however, there is a lack of scientific studies and evidence to support this claim. Aside from helping treat various diseases, its natural phytochemical constituents can also help maintain a healthy lifestyle (Teoh, 2021).



Figure 2.1 *Clinacanthus nutans* plant. Plant Source: Herb Garden, Animal Research Complex, Advanced Medical and Dental Institute, Universiti Sains Malaysia.

### 2.1.1 *C. nutans* phytochemical compounds

Various phytochemicals were identified from various solvent extracts of *C. nutans* plant. These include lupeol, stigmasterol, and myricyl alcohol (Arullappan et al., 2014; Teoh et al., 2017). From the butanol and water extracts of *C. nutans*, six C-glycosyl flavones, which are isomollupentin 7-O- $\beta$ -glucopyranoside, isoorientin,

isovitexin, orientin, schaftoside and vitexin were isolated (Tuntiwachwuttikul et al., 2004).

Satakhun et al. (2001) reported the discovery of two glycolipid compounds found in the leaves. These compounds are 1-O-palmitoyl-2-Olinolenoyl-3-O-D-galactopyranosyl-glycerol and 2-O-lipoyl-1-O-glycerol. A total of nine compounds, including a monoacylglycerol, were isolated from the leaf ethyl acetate fraction (Tuntiwachwuttikul et al., 2004). An antimicrobial compound known as 1,2-benzenedicarboxylic acid, mono (2-ethylhexyl) ester was also isolated from the chloroform leaf extract (Yong et al., 2013). Aside from having phenolic acids (caffeic acid and gallic acid), *C. nutans* extracts also have flavonoids, such as catechin and kaempferol (Ghasemzadeh et al., 2014).

Moreover, *C. nutans* contains various phytochemicals which have anti-inflammatory and antioxidant properties. Some of these include lupeol, catechin, and vitamin E. Studies on various bioactive compounds have shown that they could treat conditions such as hyperuricemia and wound healing. Among the compounds studied were isovitexin, cycloclinacoside-A1, and shaftoside (Radhakrishnan et al., 2016).

### 2.1.2 *C. nutans* pharmacological activities

The various extraction solvents used to extract *C. nutans* and their reported pharmacological activities are as summarised in Table 2.1.

Table 2.1 The pharmacological activities of *C. nutans* leaf extracts.

Extraction solvent	Pharmacological activities	Reference
Acetone	Antimicrobial properties against several pathogenic gram-positive, gram-negative strains and fungi strains.	(Kong & Abdullah Sani, 2018)
Acetone	Antiproliferative effect against Non-Hodgkin's lymphoma cells by decreasing their mitochondrial membrane potential, increasing	(Lu et al., 2018)

	reactive oxygen species and calcium ions, and upregulating the IRE-1 $\alpha$ and CHOP proteins.	
Chloroform	Antiproliferative effects against erythroleukemia (K-562), cervical cancer (HeLa), gastric cancer (SNU-1), lung cancer (NCI-H23), colon adenocarcinoma (LS-174T), hepatocellular carcinoma (HepG2), and Burkitt's lymphoma (Raji).	(Yong et al., 2013)
Chloroform and hexane	Antiproliferative effects on HepG2, nasopharyngeal cancer (CNE1) and non-small cell lung cancer (A549). Hexane extract induced sub-G1 phase arrest and oxidative stress-induced apoptosis. Upregulation of caspases 8 and 9 was observed at high concentrations (> 100 $\mu$ g/mL).	(Ng et al., 2017)
Ethanol	Neuroprotective effects on endothelial cells and astrocytes under hypoxic conditions by downregulating histone deacetylases (HDAC1/6).	(Tsai et al., 2016)
Ethanol	Antioxidant activity (protective effect) of plasmid DNA from riboflavin photoreaction.	(Yuann et al., 2012)
Ethanol and ethyl acetate extracts	Antiproliferative effects on breast cancer cells (MCF-7).	(Intan et al., 2015)
Hexane, dichloromethane and methanol	Antiviral activities against HSV-1 and HSV-2.	(Kunsorn et al., 2013)
Methanol	Anticancer effect by reducing nitric oxide and malondialdehyde levels in the blood of mice treated with 200 mg/kg and 1,000 mg/kg of leaf extract. Mitotic cells, tumour weight, and volume were decreased. No adverse or inflammatory reactions related to splenocyte activities were observed in all treated mice.	(Haron et al., 2019)
Methanol	Cytotoxic effects were found against HepG2, A549, HT-29, MDA-MB-231, MCF-7, and CRL-1739 cancer cell lines. Inhibitory activity against Cytochrome P450 (CYP3A4 & CYP2E1) in human liver microsomes.	(Quah et al., 2017)
Methanol	Induced apoptosis in human melanoma cells (D24).	(Fong et al., 2016)
Methanol	Central and peripheral antinociceptive activity by activating the opioid receptor and nitric oxide-mediated pathway.	(Abdul Rahim et al., 2016)
Methanol	Inhibited the growth of MDA-MB-231 triple-negative breast cancer cell line.	(Khiru Nasir & Mohd Bohari, 2015)
Methanol	Increased AChE activity in the liver, kidney and heart but not in the brain of male mice.	(Lau et al., 2014)
Methanol	Antibacterial activity against <i>Escherichia coli</i> and <i>Staphylococcus aureus</i> .	(Yang et al., 2013)

Methanol and water	Termination of hyperlipidemia-associated oxidative stress in rats by increasing the activity of antioxidant enzymes as well as the expression of antioxidant genes in serum and liver.	(Sarega et al., 2016)
Petroleum ether and ethyl acetate	Only petroleum ether leaf extract inhibited the growth of HeLa cells.	(Arullappan et al., 2014)
Water	Sonicated water extract had the highest nitric oxide inhibitory effect in lipopolysaccharide-interferon-gamma-induced RAW 264.7 macrophages.	(Khoo et al., 2019)
Water	Anti-angiogenic activities in endothelial cells.	(Ng et al., 2018)

## 2.2 Carbohydrates

The four major classes of organic compounds are carbohydrates, lipids, proteins, and nucleic acids. These compounds are known as polymers or macromolecules and play a vital role in the proper functioning of living organisms (Albuquerque et al., 2020). These four compounds are formed primarily by different carbon, hydrogen, and oxygen ratios. Among these, carbohydrates are the most abundant in nature. They are majorly produced by plants and algae all year round ( Xu & Queneau, 2014; Albuquerque et al., 2020). Carbohydrates are formed by the conversion of water and carbon dioxide into energy during the photosynthesis of green plants. Generally, they serve as an energy source and a structural component of organisms. Aside from being an energy source, carbohydrates are also known to contain genetic information, making up a part of nucleic acid (Davidson, 2018).

Carbohydrates simply mean ‘carbon’ and ‘water’, which contributes to the empirical formula of the simplest carbohydrate;  $[C(H_2O)]_n$ , where  $n = 3$  to  $7$  (Subrata Pal, 2020; Seeberger, 2022). Carbohydrates fall into three major structural classes: monosaccharides, oligosaccharides, and polysaccharides. These three classes are according to the number of structural units that they contain (Ouellette & Rawn, 2015).

The simplest carbohydrate that cannot be hydrolysed into smaller molecules is known as monosaccharides. These carbohydrate molecules have about three to six carbon atoms. The compounds may be either aldehydes, ketones, acetals or ketals, which yield a monosaccharide and alcohol when hydrolysed (Ouellette & Rawn, 2015). Oligosaccharides, however, are typically a few monosaccharides combined: 2 - 10. The glycosidic linkages (acetal or ketal) in oligosaccharides are broken with hydrolysis, which releases the monosaccharide units. Oligosaccharides are also known as disaccharides, trisaccharides, tetrasaccharides and so on, differing with the number of linked monosaccharide units (Ouellette & Rawn, 2015).

On the other hand, polysaccharides are usually composed of thousands of monosaccharide units linked covalently. Each polysaccharide contains a central unit that serves as the acetal/ketal centre to form a glycosidic bond to the neighbouring monosaccharide (Ouellette & Rawn, 2015). Generally, polysaccharides are divided into two subunits, homopolysaccharides or heteropolysaccharides. Homopolysaccharides are made up of only one type of monosaccharide. Heteropolysaccharides are characterised by multiple types of monosaccharides (Ouellette & Rawn, 2015). Both polysaccharides are formed by the monosaccharide units either linking in a linear fashion or branching out to form complex sugars (Xie et al., 2016).

### **2.2.1 Crude polysaccharides**

Despite the widely known properties of simple carbohydrates, the complex structure of polysaccharides remains an area of interest. In the process of isolation/extraction, polysaccharides rarely exist on their own; rather, it exists as a conjugate with other components which act as a whole (Junqiao Wang et al., 2016). Hence, crude

polysaccharides may contain small amounts of protein, phenolic compounds, and uronic acid conjugates (Ross et al., 2015).

Uronic acids are monosaccharides where the terminal hydroxymethyl group has been oxidised to a carboxylic acid. They are also essential components of many life forms, involved in the formation of various polysaccharides and glycoconjugates (Biermann, 2021; Boleij et al., 2020). Phenolic compounds are a major secondary metabolite found in plants and are separated into two; phenolic acids and polyphenols. Mono- and polysaccharides are sometimes found combined with one or more phenolic compounds or even appear as a derivative (ester or methyl esters) (Minatel et al., 2017).

Generally, the bioactivities of crude polysaccharides outweigh the bioactivities of purified polysaccharides. There have been claims that the antioxidant activity of crude polysaccharides was reduced dramatically upon fractionation and purification of the plant polysaccharide. These studies suggested the possibility that the other compounds present in the crude polysaccharide extract (such as pigments, proteins and polyphenols) were contributing to the higher antioxidant activity (Fan et al., 2014; Wu et al., 2014).

Crude polysaccharides also showed pronounced antioxidant activity in DPPH radical scavenging assays, which could be due to the polyphenolic-associated polysaccharide fraction that is formed between the polysaccharides and the high molecular weight phenolics. A study revealed that the phenolic and protein content of three different mushroom species (*Lentinula edodes*, *Grifola frondosa*, and *Trametes versicolor*) were significantly correlated with elevated antioxidant activities (Siu et al., 2014). Nevertheless, phenolic and protein-free purified polysaccharides barely showed antioxidant activities. Hence, crude polysaccharides with some amount of phenolic

compounds conjugated might be the reason for the increased antioxidant potential compared to purified polysaccharides.

Additionally, scientific investigations related to polysaccharide technology are needed to develop new approaches for the exploitation of its potential in the development of biocomposite, nano-conjugate, and pharmaceutical delivery systems. Even though different formulations may have different properties, polysaccharides are still superior to other polymers when it comes to terms of ease of use, non-toxicity, biocompatibility, and biodegradability (Gopinath et al., 2018).

### **2.2.1(a) Extraction of water-soluble crude polysaccharides from plants**

Water extraction of polysaccharides is the most common, easily accessible, and safe method of extraction used in the food industry (Jing et al., 2016). Basically, the efficiency of polysaccharide extraction and yield is influenced by several factors, including the extraction time, temperature and water-to-extract ratio (Shang et al., 2017). Most plant polysaccharides are composed of structural constituents that can be extracted from the cell walls. The various methods used for extracting these constituents vary depending on the structure of the cell (Chen et al., 2021). Some commonly used water extraction methods include hot water extraction, acidic extraction, and dilute alkaline extraction method.

Recently, enzymatic and physical extraction methods, including freeze-thaw, microwave and ultrasonic extraction methods, have also been applied with much success in the extraction of plant polysaccharides (X. Ma et al., 2017). Then the isolation of crude polysaccharides is done by alcohol precipitation. Since polysaccharides are not soluble in alcohol, further washing steps done with pure alcohol would remove residues from the crude polysaccharide. The percentage yield



and the bioactivity of all plant polysaccharides vary based on the extraction and isolation procedure used (Chen et al., 2021).

Among the extraction methods, the ultrasound-assisted extraction method is commonly used for the extraction of various substances. Due to its numerous physical effects, ultrasound waves could effectively and quickly diffuse into the plant cell and release the active components into the solvent, making it favourable in the extraction of polysaccharides. Generally, ultrasound-assisted extraction improves the extraction rate and extraction time (X. Ma et al., 2017). This was attributed to the fact that ultrasonication increased the protein content in crude polysaccharides (Mtetwa et al., 2020).

Alkaline and acidic extraction methods yield alkaline-soluble and acid-soluble polysaccharides, respectively. A number of studies suggested that acidic extraction methods allowed higher yields of low molecular weight polysaccharides by hydrolysing the glycosidic bonds (Gao et al., 2017; Yao et al., 2017; Sun et al., 2018). Nevertheless, there are several studies that suggest the alkaline extraction method is efficient in obtaining polysaccharides rich in bioactivities (Zhang et al., 2013; Khodaei et al., 2016; Ma & Mu, 2016). A study conducted using polysaccharides extracted from *Lonicera japonica* (LJP) reported that the extraction yield of the polysaccharides from an alkaline solution was higher than that of acidic or water extraction methods (Sun et al., 2018). This study suggested that all three extractions (LJP- Acid, LJP-Alkali and LJP-Water) were rich in uronic acid content and fucose but had different molecular weights, structures, colours and were made up of different monosaccharides. Besides, LJP-Alkali exhibited the most advantageous properties when subjected to ion chelating studies on egg yolk homogenates, suggesting the inhibition of lipid peroxidation (Zhu et al., 2016). Based on several studies, crude polysaccharides

extracted via alkaline and acidic methods seem to have more potent biological activities and produce a higher yield of polysaccharides (Sun et al., 2018).

One study conducted to explore the impact of the extraction pH on the extracted polysaccharide yield from peanut sediment of an aqueous extraction process reported that the yield was significantly higher at acid (pH 4) and alkali (pH 12). As the pH decreased from 2 - 6, the yield increased. At acidic pH (pH 4), a breakage of the biopolymer glycosidic bonds by hydrogen ions from HCl was the main reason for the dissolving of the polysaccharides. However, at pH 6, the temperature was predominantly responsible for breaking the biopolymer structures. Moreover, an increase in the extraction pH from 8 to 12 enhanced the dissolution of proteins and thereby raised the yield (Ye et al., 2019).

### **2.2.1(b) Solubility**

Monosaccharides are polar molecules with several -OH functional groups that are responsible for their hydrophilic nature. Besides, monosaccharides have a lower solubility in organic solvents compared to water (Istasse & Richel, 2020). Polysaccharides, however, have a diverse range of solubility; some are water-insoluble (cellulose), some are insoluble in cold water (starch); and some are insoluble in hot water (pullulan and gum Arabic) (Guo et al., 2017). Nevertheless, due to the multi-OH groups, polysaccharides have a strong affinity for water molecules. This can cause polysaccharides to interact with each other through hydrogen bonding. Polysaccharide solubility depends solely on the interaction between molecule-molecule and molecule-solvent. In water-soluble polysaccharides, the favourable interaction is between water and polysaccharide molecules, where the solvent forms a solvating envelope enclosing the polymer chain. This causes the polysaccharide molecules to be apart from each other (Guo et al., 2017).

For poorly water-soluble polysaccharides, the intermolecular interactions between the polysaccharide polymer segments can lead to aggregation and eventually to gelation. Under certain conditions, the interaction between the polysaccharide polymers and the water molecules can compensate for the polymer-water interaction; this is known as the theta condition. In theta condition, the chain conformation is defined by the bond angles and the short-range interactions that occur between the polymer coil dimension and the bond (Guo et al., 2017). The solubility of polysaccharides depends on their molecular structures. Higher solubility is linked to structural features that inhibit the formation of intramolecular associations, which includes charged groups (carboxylate, phosphate and sulfate groups) and branching structures. In contrast, lower solubility is linked to structural features that elevate the intramolecular associations, including large molecular weight and linear chain (Guo et al., 2017).

Therefore, polysaccharide structural features play a crucial role in determining the solubility of the sugar. In an ethanol-water solution, the soluble properties of the polysaccharides decreased as the ethanol content increased. The results also showed that the soluble properties of the oligosaccharides were minimal in pure ethanol (Guo et al., 2017). This explains the precipitation and washing steps of carbohydrates using pure ethanol during the extraction procedure.

### **2.2.1(c) Antioxidant activities**

The presence of protein and pigments in alkaline-soluble and water-soluble crude polysaccharides from *Inonotus obliquus* could influence the radical scavenging effects (Mohanta et al., 2022). It has also been hypothesised that the radical scavenging ability of polysaccharide molecules is linked to the number of hydroxyl groups in their polysaccharides (Zhao et al., 2013). Numerous studies reported that crude

polysaccharide extracts exhibited potent antioxidant activities as compared after further fractionation, which yielded purified polysaccharides. Purified polysaccharides yield low to moderate activity, which suggests that the presence of a small number of other plant compounds, including proteins and polyphenols, contributes to the increased antioxidant activity (Cheng & Huang, 2018; Hamed et al., 2020; Huo et al., 2022).

In 2013, a study on the crude polysaccharides of tea extracts was tested to identify the role of the polyphenols present in order to evaluate the antioxidant capabilities. This study concluded that the crude tea polysaccharides exhibited potent antioxidant activities as compared to the further purified polysaccharide fractions, which hardly exhibited any antioxidant activity. This study suggested that in the presence of polyphenols, the DPPH radical scavenging ability was enhanced, indicating that polyphenols triggered a synergistic elevation in the antioxidant activity (Wang et al., 2013). Another study conducted to compare the antioxidant activity of crude, and purified fractions of polysaccharides from the plant *Dendrobium officinale* reported that the DPPH scavenging activity was significantly higher in crude polysaccharides. They suggested the reason for the higher antioxidant content could possibly be due to the presence of other compounds, including polyphenols, proteins and microelements (Zhao et al., 2013). A similar study was conducted, with similar results, indicating the increase in antioxidant activity in crude polysaccharides from *Fritillaria pallidiflora* could possibly be due to the protein present in them (Rozi et al., 2019).

Furthermore, acidic extracted crude polysaccharides are considered efficient antioxidants due to the presence of uronic acids, which are believed to be key components contributing to the antioxidant activity in polysaccharides (Al-Sheraji et

al., 2012; Hui et al., 2013). Acidic polysaccharides has a higher concentration of hydrogen ions making aldehydes or ketones oxidise easily (Jiang et al., 2021). One study elucidated that the antioxidant activity, including DPPH radical scavenging and FRAP on glucuronic acid, galacturonic acid, and polygalacturonic acid, exhibited potent antioxidant activity, with the highest activity reported in polygalacturonic acid. The researchers concluded that the nature of the polymerisation might be the reason for the difference in activity (Rao & Muralikrishna, 2006).

### 2.3 Metabolomics

The omics approach and hierarchy are shown in Figure 2.2. Metabolomics is a scientific study of the products and substrates of metabolism. The metabolism of a living organism is affected by both its environment and genetic factors. Therefore, metabolomics is a quantitative technique that allows the identification and quantitation of the various metabolites that play a role in the metabolism of living organisms (Alseekh et al., 2021; Clish, 2015).

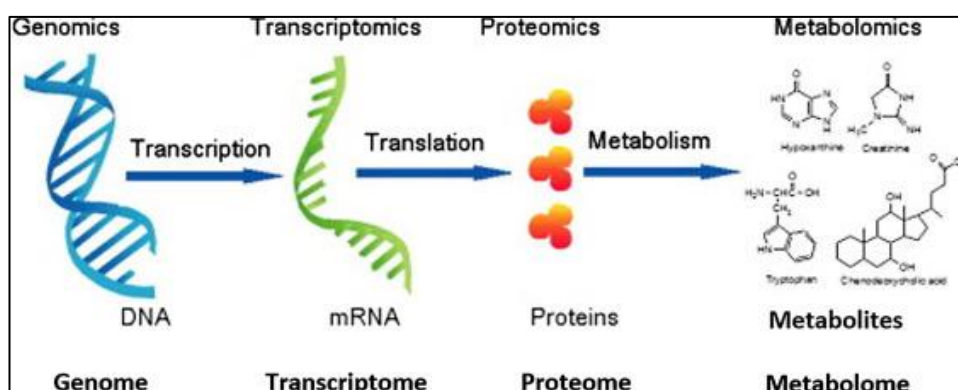


Figure 2.2 Omics approach and hierarchy. Extracted from Frueh & Burczynski (2020).

Metabolomics is an upcoming field used for various applications; including for comparing mutants (Clark et al., 2019), assessing responses to environmental stress (L. J. Zhang et al., 2021), studying global effects of genetic manipulation (Bragagnolo

et al., 2021), toxicology evaluations (Olesti et al., 2021), nutritional epidemiology (Brennan et al., 2021; Levatte et al., 2022), cancer pharmacology (Liang et al., 2021), drug discovery (Tounta et al., 2021; Alarcon-Barrera et al., 2022) and natural product discovery (Caesar et al., 2021; Tsugawa et al., 2021). There are three main approaches used for metabolomics studies: metabolic profiling which is divided into targeted analysis and un-targeted analysis, as well as metabolic fingerprinting (Onuh & Qiu, 2021). The advantages and disadvantages of these major approaches are shown in Table 2.2. Targeted approaches require prior knowledge of the molecule(s) of interest to design tailored analytical methods. Nevertheless, the establishment of extensive targeted methods has been facilitated by the increasing availability of metabolite libraries (e.g., IROA technologies) (Han et al., 2021). Untargeted approaches aim to detect as many metabolites as possible in a sample with subsequent annotation and identification, usually involving database searches (e.g., METLIN or MS-DIAL) (Tsugawa et al., 2015) as well as comparison with authentic synthetic materials (Salek et al., 2013).

Table 2.2 Advantages and disadvantages of the major approaches in metabolomics. Adapted from Fraga-Corral et al. (2022).

<b>Approach</b>	<b>Advantage</b>	<b>Disadvantage</b>
Metabolic profiling (targeted)	<ul style="list-style-type: none"> <li>• Quantitative</li> <li>• Low limit of detection</li> <li>• High throughput</li> </ul>	<ul style="list-style-type: none"> <li>• Limited number of compounds can be targeted</li> <li>• Does not detect compounds that were not targeted</li> <li>• Targeted compounds must be available and purified for calibration</li> </ul>

Metabolic profiling (un-targeted)	<ul style="list-style-type: none"> <li>• Global (not targeted)</li> </ul>	<ul style="list-style-type: none"> <li>• Semi-quantitative</li> <li>• Majority of peaks are not identifiable</li> <li>• Difficult informatics</li> <li>• Medium throughput</li> </ul>
Metabolic fingerprinting	<ul style="list-style-type: none"> <li>• Global (not targeted)</li> <li>• Directly applicable to pattern recognition</li> <li>• Highest throughput</li> </ul>	<ul style="list-style-type: none"> <li>• No compound identification</li> </ul>

Plant metabolomics is a branch of metabolomics designed to study the overall changes in a large number of metabolites in plant samples and then conduct deep data mining and bioinformatic analysis (Xiao et al., 2022). Plant metabolites are components of defence systems developed by plants in response to pathogen attacks and other environmental stresses. They are an important source of many natural pharmacological activity products which are often designated as specific biological activities associated with their biochemical structures (Lu & Cui, 2019).

Metabolite profiling is the commonest technique used for assessing the level of metabolites in samples. The identification of plant metabolites is associated with a series of events, including the experimental design, sample collection, sample processing, sample preparation, detection, analysis and data processing (Salem et al., 2020). Analytical techniques and data processing techniques are the two major parts of metabolomics. Table 2.3 illustrates the analytical techniques together with their advantages and disadvantages in metabolite profiling. The data processing techniques are reviewed in Section 2.8.2 (b).